

# Supporting Information

## Efficient Radical-Driving Electrocatalytic Dimerization of Furfural to Jet Fuel Precursors using WMoB Nanoflakes

*Xiaodie Zhang<sup>a</sup>, Bin Liu<sup>a</sup>, Yuchen Wang<sup>a</sup>, Ying Long<sup>b,\*</sup>, Zhenhao Xu<sup>a</sup>, Hua-Tay Lin<sup>b</sup>,  
Rafael Luque<sup>c,d,\*</sup>, Kai Yan<sup>a,\*</sup>*

<sup>a</sup> Guangdong Provincial Key Laboratory of Environmental Pollution Control and Remediation Technology, School of Environmental Science and Engineering, Sun Yat-sen University, Guangzhou 510275, China

<sup>b</sup> State Key Laboratory for High-Performance Tools, School of Electromechanical Engineering, Guangdong University of Technology, Guangzhou 510006, China

<sup>c</sup> Peoples Friendship University of Russia (RUDN University), 6 Miklukho Maklaya str., 117198, Moscow, Russian Federation

<sup>d</sup> Universidad ECOTEC, Km. 13.5 Samborondón, Samborondón, EC092302, Ecuador

\* Email: [yinglong@gdut.edu.cn](mailto:yinglong@gdut.edu.cn) (Ying Long), [rluque@ecotec.edu.ec](mailto:rluque@ecotec.edu.ec) (Rafael Luque), [yank9@mail.sysu.edu.cn](mailto:yank9@mail.sysu.edu.cn) (Kai Yan).

#These authors contributed equally to this work.

## Supplementary Figures, Schemes and Tables

### DFT calculation method

All calculations were conducted using the CP2K package (version 7.1) within the framework of density functional theory, employing a hybrid Gaussian and plane-wave approach. The PBE functional was used for electronic structure calculations. The molecular orbitals of valence electrons were expanded with DZVP-MOLOPT-SR-GTH basis sets, while atomic core electrons were described using Goedecker-Teter-Hutter pseudopotentials. A plane-wave density cutoff of 500 Ry was applied. The long-range van der Waals interactions were accounted for using the DFT-D3 method. To prevent artificial interactions between periodic images, a 15 Å vacuum layer was introduced perpendicular to the sheet. The K-point mesh was set to  $2 \times 2 \times 1$ . Structural relaxation was performed using the BFGS algorithm within CP2K, with a force convergence threshold of  $4.5 \times 10^{-4}$  hartree/bohr.

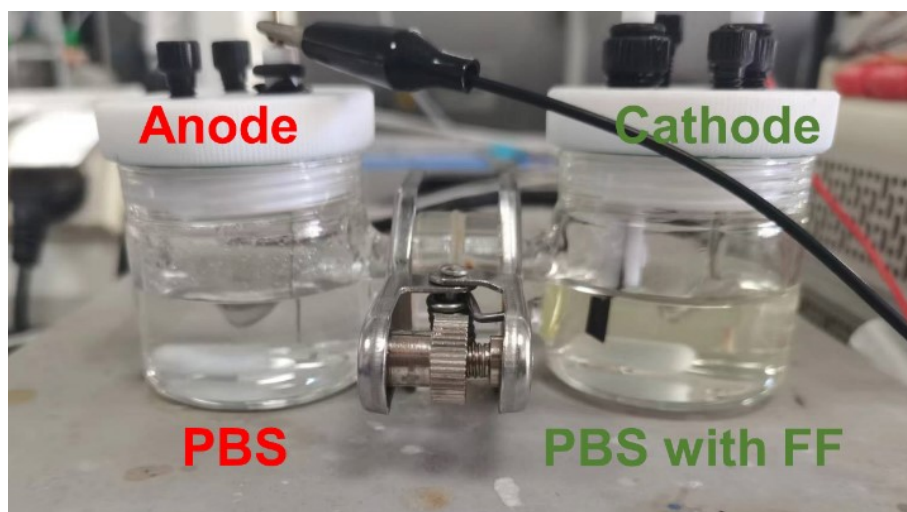


**Figure S1.** H-type cell containing 30 mL PBS (left) and FF (right)

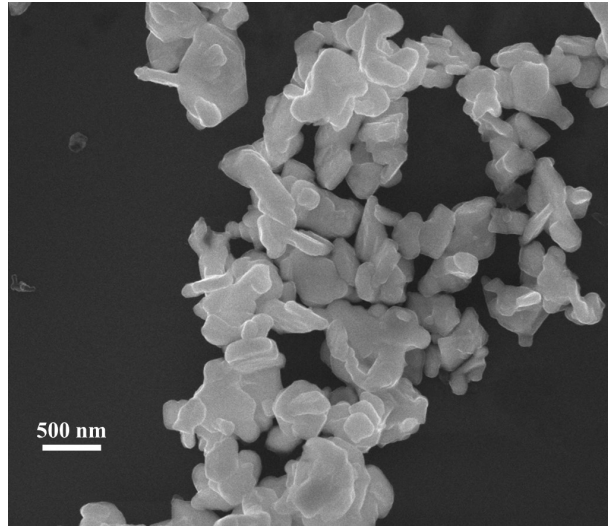


**Figure S2.** SEM of WMoB nanoflakes.

**Table S1.** Elemental analysis of WMoB by ICP-OES (Agilent 5110)

Elements	Element content (%)
B	15.0020%
Mo	2.9737%
W	81.6095%

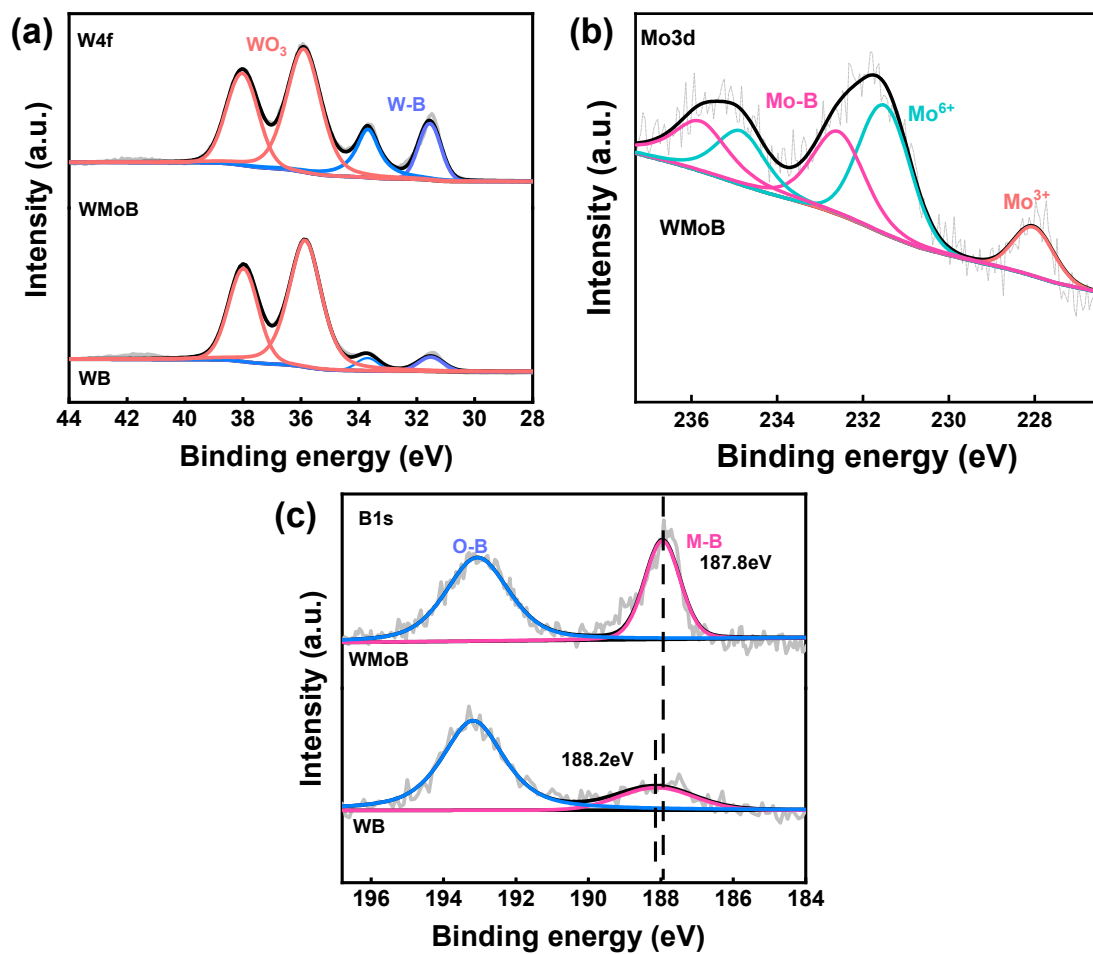
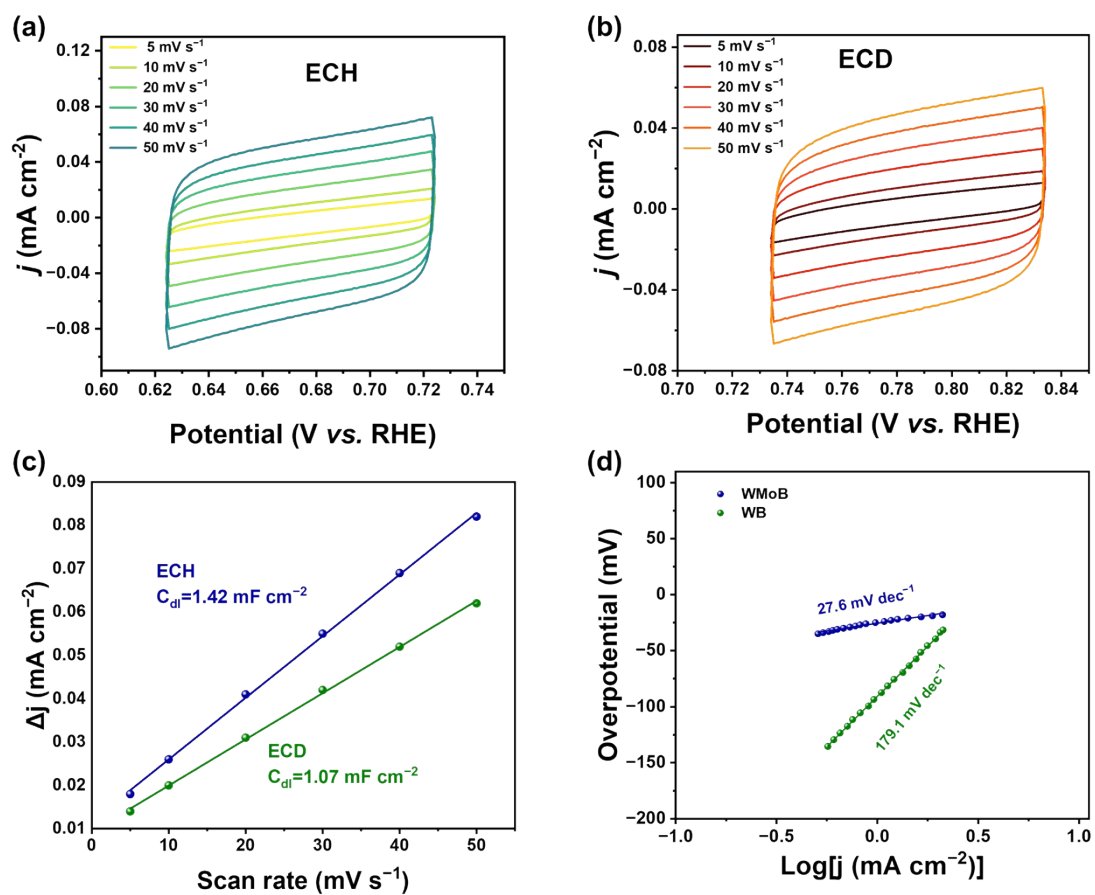
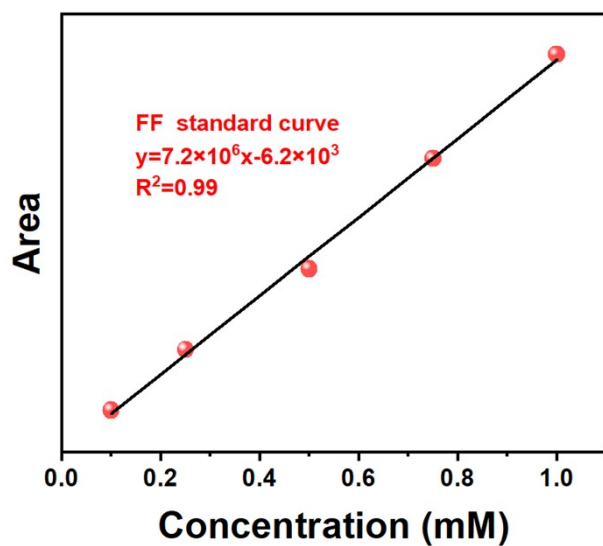


Figure S3. XPS survey spectra of WMoB nanoflakes and WB.



**Figure S4.** Electrochemical performance. The relationship between current and scan rate (5–50 mV s<sup>-1</sup>) was obtained from the CV curves. (a) ECH and (b) ECD. (c) The  $C_{dl}$  was collected by cyclic voltammetry at different scan rates. (d) The Tafel slopes of WB and WMoB nanoflakes.



**Figure S5.** HPLC standard curves of FF.

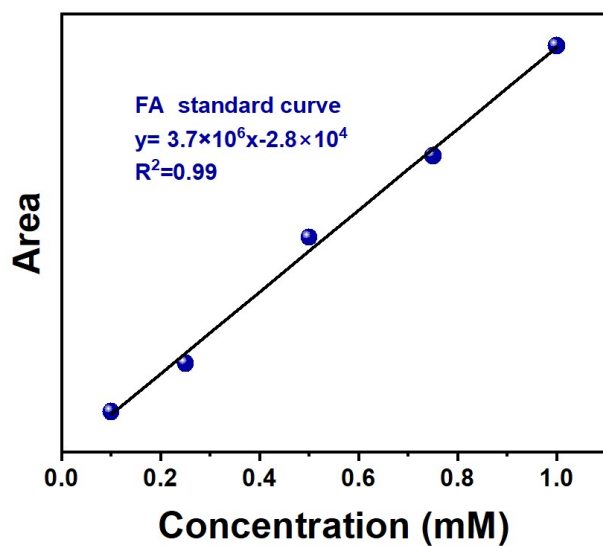


**Figure S6.** HPLC standard curves of FA.

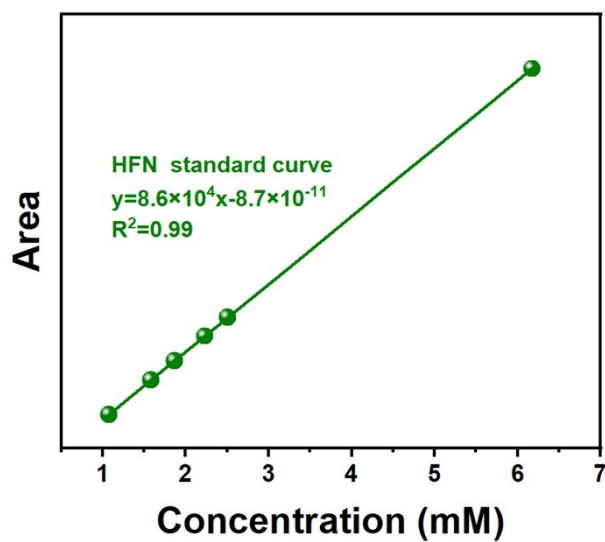


**Figure S7.** NMR standard curves of HFN.

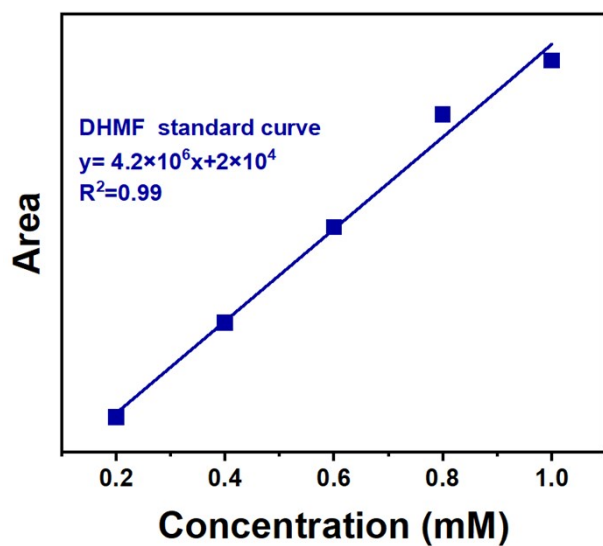


**Figure S8.** HPLC standard curves of DHMF.

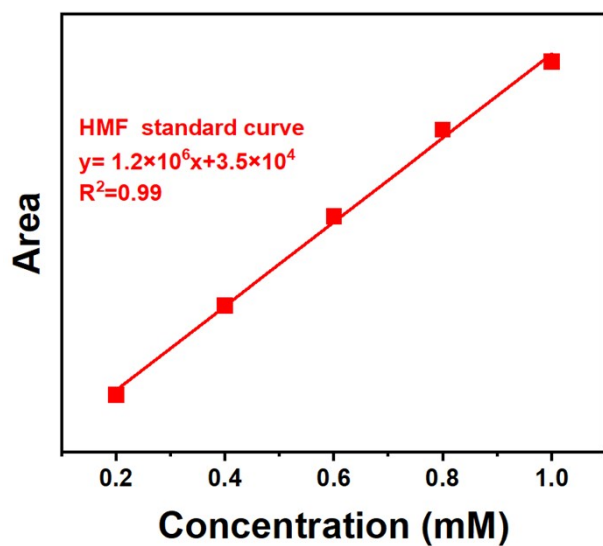


**Figure S9.** HPLC standard curves of HMF.

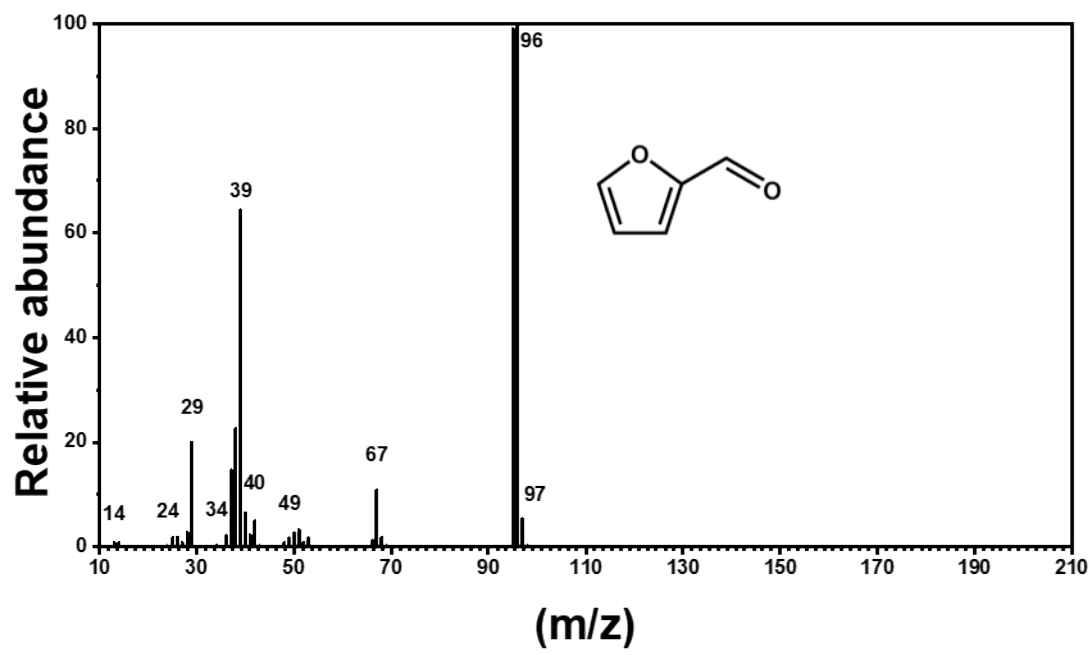


Figure S10. Mass spectra of FF.

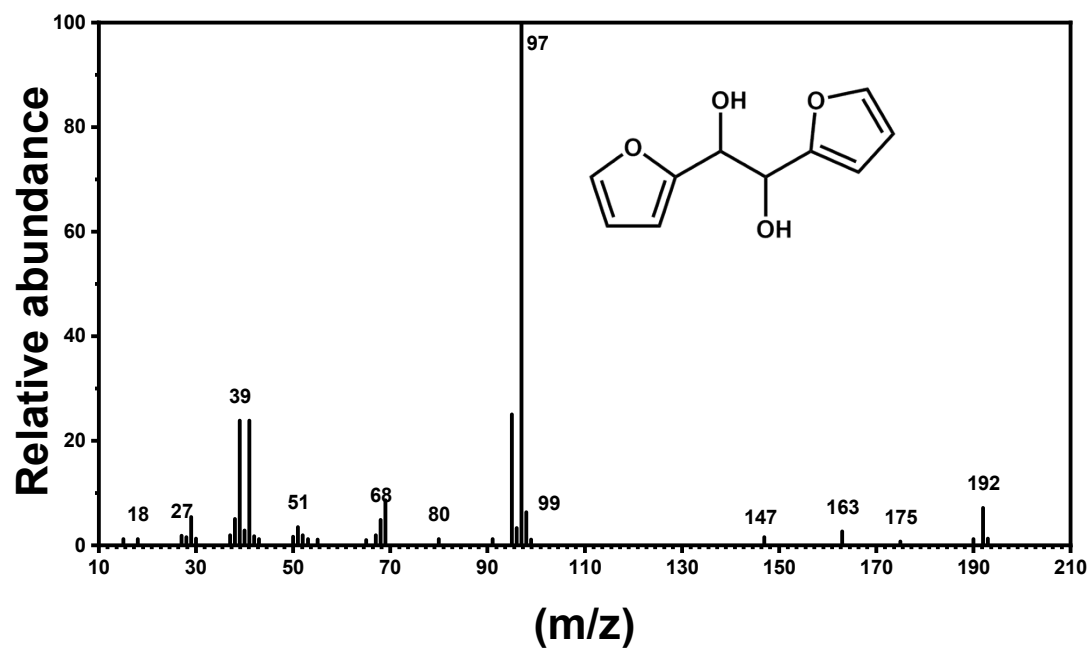


Figure S11. Mass spectra of HFN.

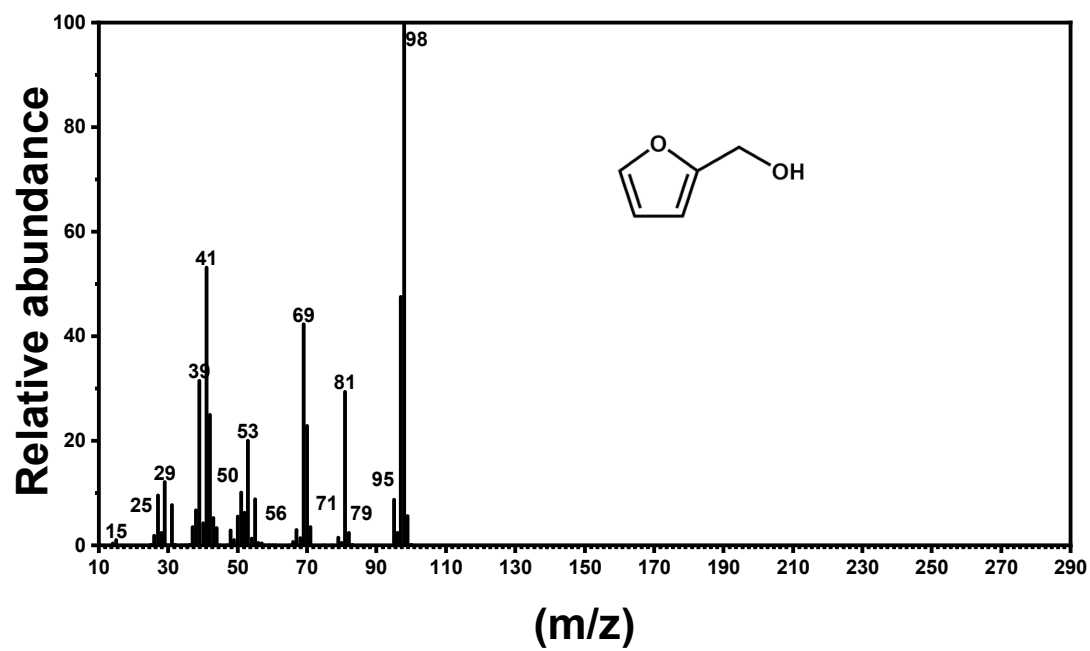
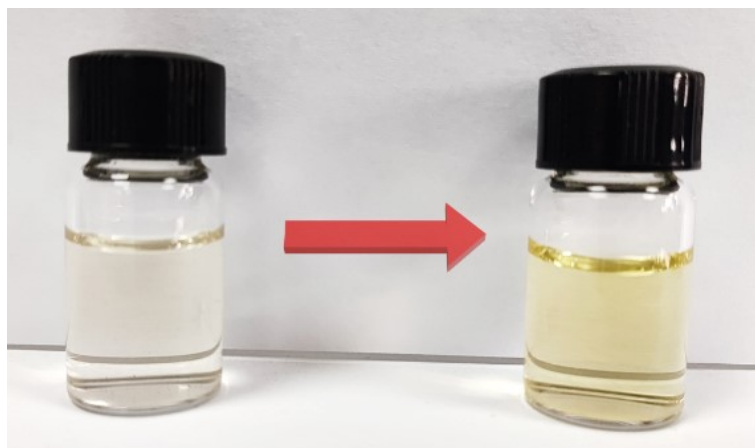
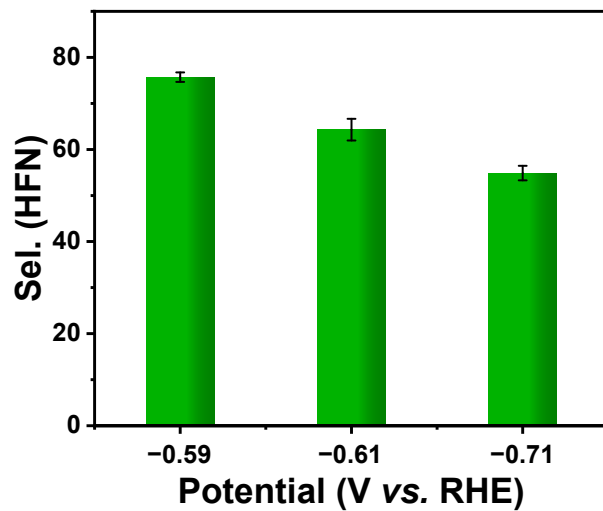


Figure S12. Mass spectra of FA.



**Figure S13.** Original sample (left) and post-reaction sample (right).



**Figure S14.** The selectivity of WMoB nanoflakes for HFN with error bars at different potentials.

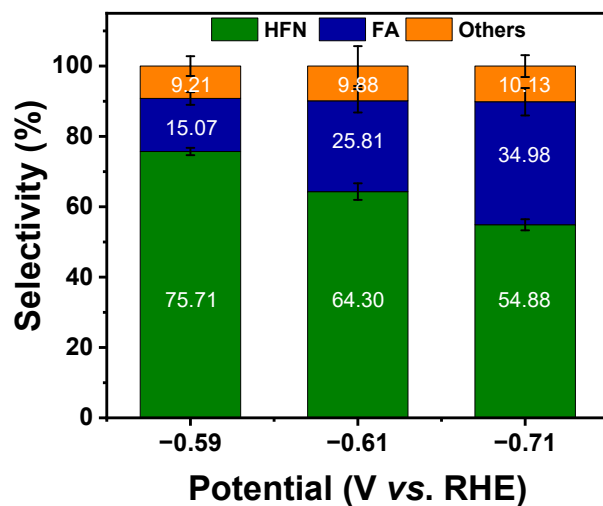


**Figure S15.** The selectivity for different products with error bars of WMoB nanoflakes at different potentials.

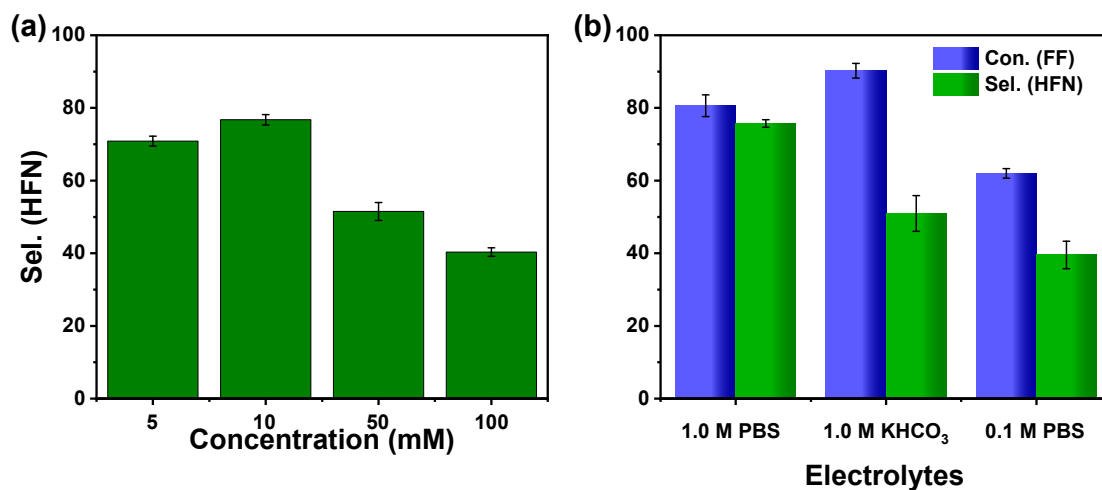


**Figure S16.** (a) The selectivity of HFN with error bars under different FF concentrations; (b) The conversion for FF and selectivity for HFN of WMoB nanoflakes with error bars in different electrolytes.

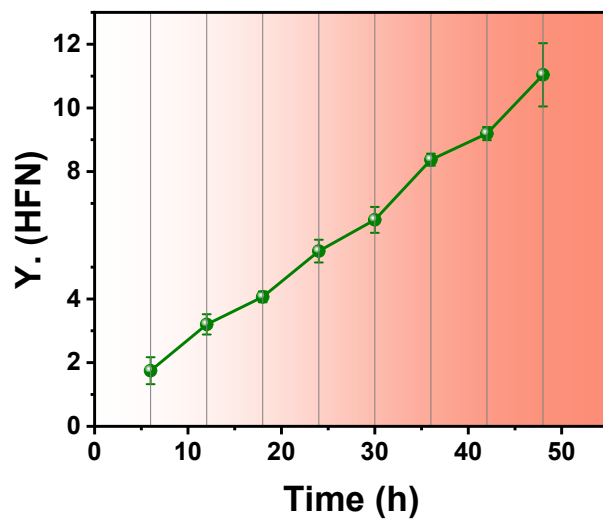


**Figure S17.** Cumulative concentration of HFN generated during long-term electrolysis over 48 h..

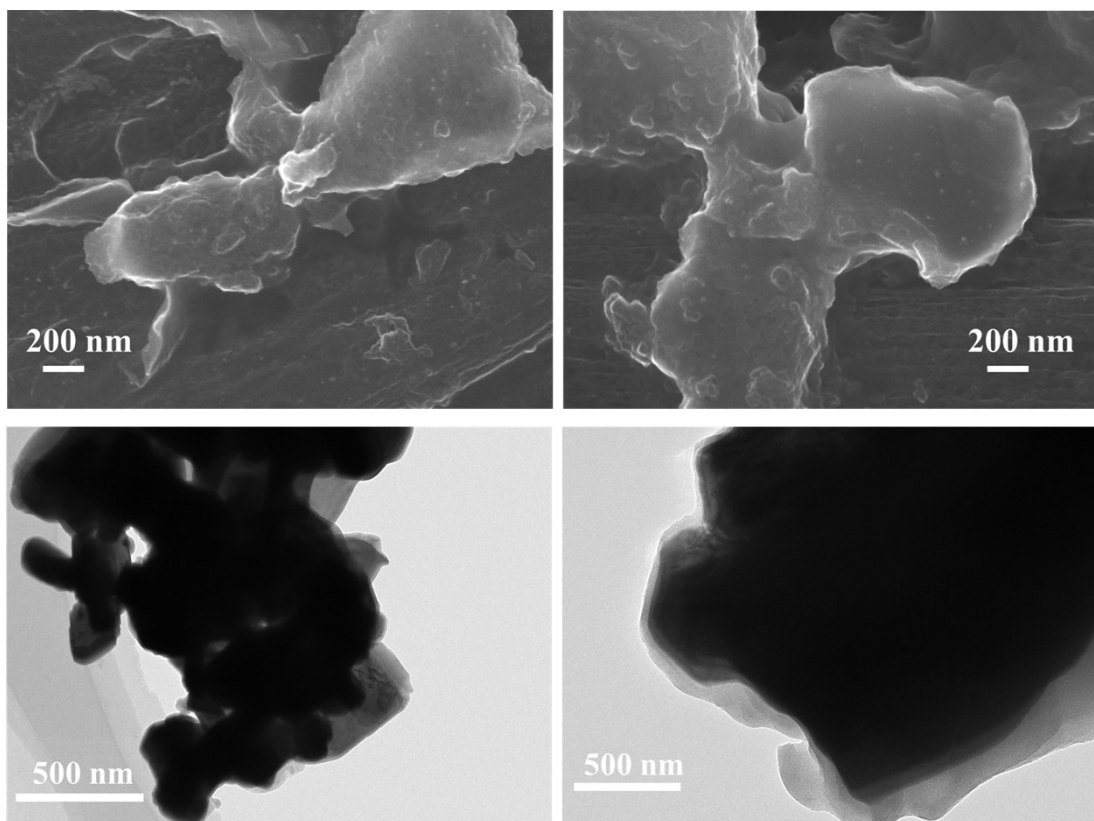


**Figure S18.** SEM and TEM of WMoB nanoflakes after the reaction.

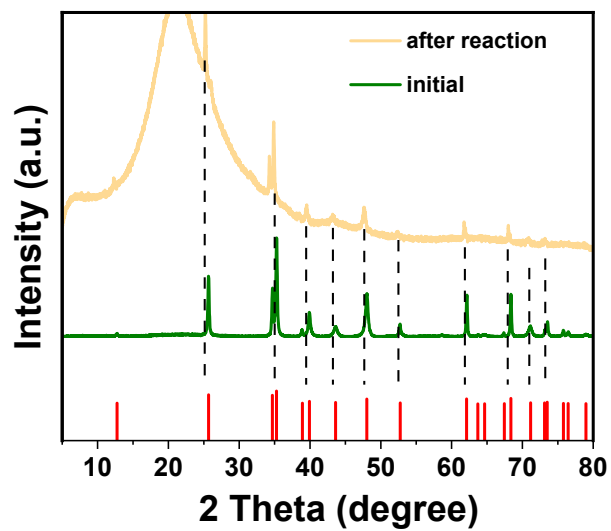


**Figure S19.** Comparison of XRD patterns of WMoB nanoflakes before and after the reaction.

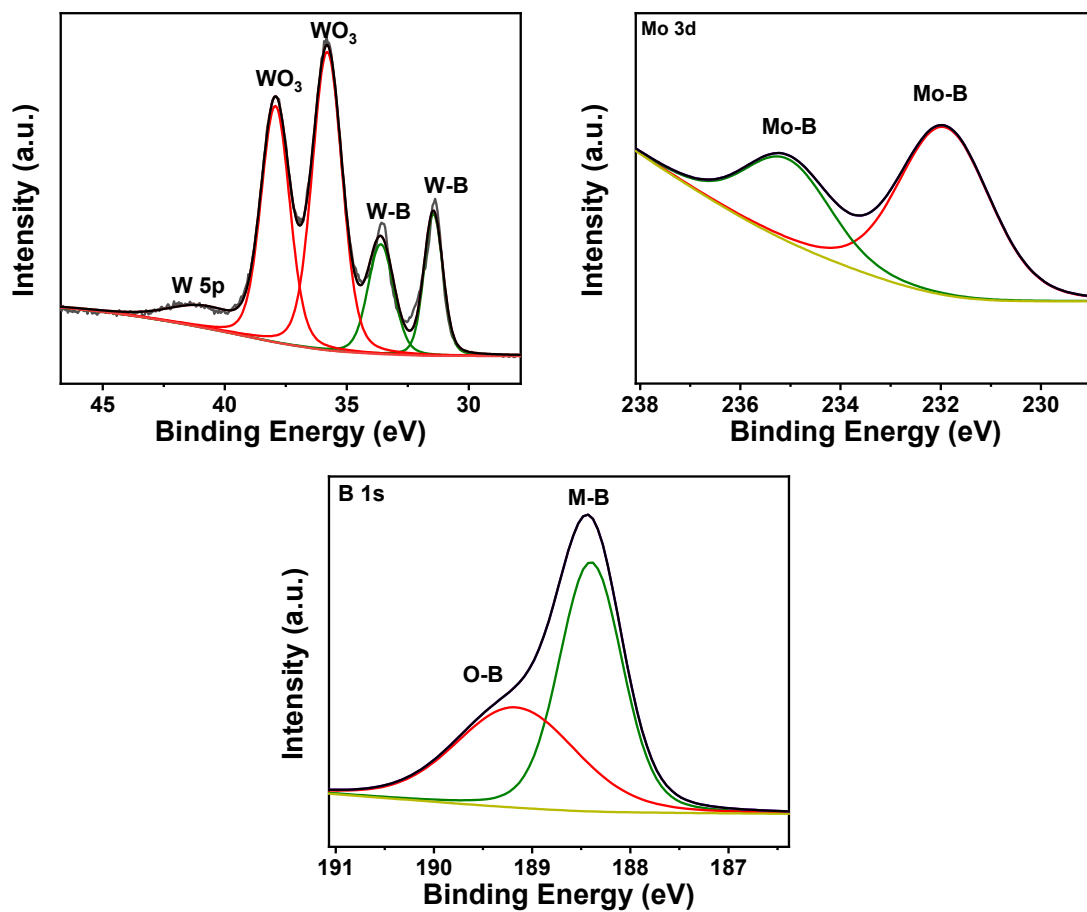


**Figure S20.** The XPS spectrum of WMoB nanoflakes after the reaction.

**Economic analysis:**

To evaluate the practical potential of the ECD process, a simplified economic analysis was carried out based on a standard experiment involving 30 mL of 1.0 M PBS under a constant potential of  $-1.3$  V. In this system, FF was introduced at a concentration of 10 mM. Given that two FF molecules were required to form one molecule of HFN, the theoretical concentration of HFN produced was calculated to be 3.8 mM, corresponding to a yield of  $1.2 \times 10^{-4}$  mol HFN  $\text{h}^{-1}$ . Based on its molecular weight (192.2 g  $\text{mol}^{-1}$ ), the hourly production of HFN was estimated to be approximately 21.8 mg. At a market price of \$800  $\text{g}^{-1}$ , the value of the product was determined to be \$17.44  $\text{h}^{-1}$ . These results highlight the promising economic potential of FF-to-HFN conversion via the ECD process under mild and energy-efficient conditions.

**Table S2.** Comparison of FF conversion along with selectivity of HFN

Catalyst	Potential (V vs RHE)	Electrolyte	FF (mM)	Sel <sub>HFN</sub>	Refs
ed-Ag/NF	-0.45	0.5 M NaOH	50	47.2	2
Cu-Ni/NF	-0.45	0.5 M NaOH	10	15.8	2
Cu foil	-0.55	0.5 M Sulphate solution (pH = 3) with CH <sub>3</sub> CN (1:4 v/v%)	50	6.5	3
MoS <sub>2</sub>	-0.47	0.4 M sodium borate buffer with methanol (1:4 v/v%)	20	28.96	4
CuSn	-0.55	0.1 M phosphate buffer (pH=6.8)	20	60	5
WMoB	-0.59	1 M phosphate buffer (Ph=6.55)	10	76.67	<b>This work</b>

## References

- 1 S. Grimme, J. Antony, S. Ehrlich and H. Krieg, *J. Chem. Phys.*, 2010, **132**, 154104.
- 2 R. J. Dixit, K. Bhattacharyya, V. K. Ramani and S. Basu, *Green Chem.*, 2021, **23**, 4201-4212.
- 3 X. H. Chadderton, D. J. Chadderton, J. E. Matthiesen, Y. Qiu, J. M. Carraher, J. P. Tessonnier and W. Li, *J. Am. Chem. Soc.*, 2017, **139**, 14120-14128.
- 4 S. Huang, B. Gong, Y. Jin, P. H. L. Sit and J. C.-H. Lam, *ACS Catal.*, 2022, **12**, 11340-11354.
- 5 X. Liu, Y. Sun, H. Ren, Y. Lin, M. Wu and Z. Li, *ACS Catal.*, 2024, **14**, 5817-5826